Unified Network Model for Diffusion of Condensable Vapors in Porous Media

Pavol Rajniak and Ralph T. Yang
Dept. of Chemical Engineering, State University of New York at Buffalo,
Buffalo, NY 14260

A unified network model is formulated for predicting effective Fickian diffusivities of condensable vapors in porous media where capillary condensation and adsorption–desorption hysteresis occur. The model unifies the equilibrium theory based on the pore-blocking interpretation of hysteresis in the interconnected network of pores and the percolation model of mass transport in the network with randomly interspersed regions for capillary condensation and surface flow. The Bethe network is used to represent the porous medium, and the effective medium theory is employed to obtain the effective diffusivity. Using the information on the connectivity and the positions of the closure points of the hysteresis loop enclosed by the equilibrium primary adsorption and primary desorption isotherms, the concentration dependence of the effective diffusivity is predicted. The model is applied to the systems water vapor-silica gel, water vapor-activated alumina, and literature data. It successfully predicts the concentration dependence of the effective diffusivity in the whole range of relative pressures for systems both with and without a peak in the diffusivity.

Introduction

The problem of predicting diffusion rates of the adsorbable vapors in porous media in the range of pressure where capillary condensation occurs is a significant one for the design and operation of adsorbers, dryers, catalytic reactors, membrane separators, and so forth. For adsorption at subcritical temperatures, that is, for adsorption of condensable vapors, the vapor in the adsorbent exists as adsorbed molecules on the solid surface, condensed in fine pores and as vapor in the voids. At low partial pressures, monolayer adsorption plays the major role. At higher partial pressures the role of multilayer adsorption becomes important and simultaneously capillary condensation in the finer pores commences. The extent of capillary condensation increases with increasing relative pressure of the adsorptive, and eventually the entire pore volume is filled by capillary condensate. For systems with capillary condensation, type IV isotherm (Gregg and Sing, 1982) is typical, as shown in Figure 1a. The adsorbable component can be transferred by surface diffusion caused by a gradient of chemical potential, by capillary flow caused by a gradient of capillary pressure, and by the gaseous diffusion caused by a vapor-phase pressure gradient.

In spite of its practical importance, theoretical and experimental studies on the transport under these conditions are relatively limited. The study is complicated by the difficulty of separating the contributions from the various transport mechanisms. Moreover, the existing experimental results and theoretical interpretations on the transport of adsorbable vapors in the capillary condensation regime are widely different.

Various experimental methods have been used to determine the diffusivity or permeability in the capillary condensation regime. These methods (Kapoor et al., 1989) include the steady-state permeation method (Rhim and Hwang, 1975; Lee and Hwang, 1986; Abeles et al., 1991), time-lag permeation method (Gilliland et al., 1958; Tamon et al., 1981; Toei et al., 1983), and transient gravimetric method (Haynes and Miller, 1982).

Also the theoretical approaches explaining the experimental results are different. The "hydrodynamic models" (Flood et al., 1952; Gilliland et al., 1958; Haynes and Miller, 1982; Kapoor et al., 1989) can explain certain experimental results by proposing that the transport is multilayer surface flow

Correspondence concerning this article should be addressed to R. T. Yang who is currently at the Dept. of Chemical Engineering, University of Michigan, Ann Arbor, MI 48109.
Present address of P. Rajniak: Dept. of Chemical Engineering, Slovak Technical University, 812 37 Bratislava, Slovakia.

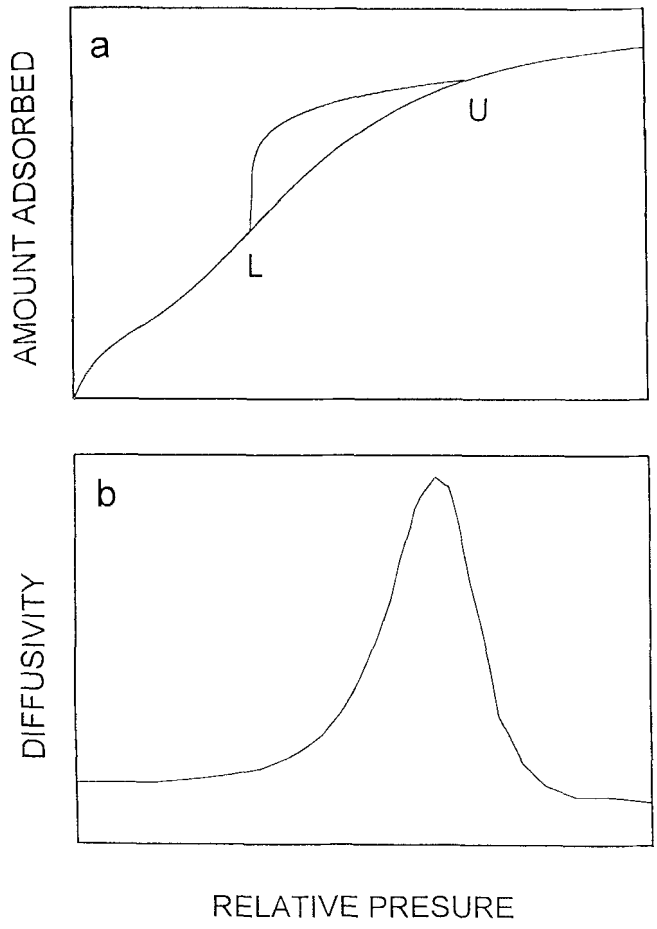

Figure 1. (a) Typical adsorption–desorption equilibrium with hysteresis loop (*L* and *U* are the closure points of the main hysteresis loop); (b) corresponding concentration dependence of diffusivity (with a maximum).

alone even in the region of coexistence with capillary condensation. There are, however, some experimental results in the capillary condensation region that cannot be interpreted by the hydrodynamic model (Tamon et al., 1981).

The transport model taking into account the hopping behavior of molecules adsorbed in the adsorbed phase and the viscous flow of the capillary condensate described by the modified Kozeny–Carman equation for the flow of fluid through porous media (Tamon et al., 1981; Toei et al., 1983) is relatively complex and requires the estimation of constants, the physical interpretation of which is tenuous.

The models mentioned earlier cannot explain one of the most interesting experimental observation on the subject—the occurrence of a maximum (or peak) in permeability or diffusivity in the capillary condensation region (Figure 1b) (Eberly and Vosberg, 1965; Rhim and Hwang, 1975; Lee and Hwang, 1986; Uhlhorn et al., 1992; this work).

To explain this experimental fact, Lee and Hwang (1985) developed a flow model by considering the blocking effect of the adsorbed phase on the basis of a cylindrical capillary structure. Six different flow modes in a capillary were considered depending on the pressure distribution and the film thickness of the adsorbed layer. In the range of capillary condensation pressures, the mechanism of adsorbed layer transport is believed to be of a hydrodynamic nature. Their model predicts the maximum peak in permeability of condensable vapors through a porous medium. However, their treatment is restricted to the idealized case of a single pore size, and the complexity caused by the pore size distribution is not discussed.

All models discussed earlier represent the classic approach to describing complex porous materials referred to as continuum models (Sahimi et al., 1990). Continuum models are often not adequate for many systems of engineering interest, for example, for systems consisting of phases that differ appreciably from one another in their effective properties. In the continuum model, the porous material is treated as a continuum within which the properties of fluid and solid species are defined as smooth functions of time and position.

In the discrete model considered in this work, the porous material is treated as a collection of pores connected together to form a network. The model formulated in this work is based on the network representation of the pore spaces and also the ideas and concepts in statistical physics of disordered media such as percolation concepts. The pore networks of catalysts are complex, and in practice it is necessary to adopt a simplified model that reproduces the main features of a real network, but ignores many of the details. The model should contain a description of both the geometry and the topology of the pore spaces. Thus, one needs a simplification of both the individual pore structure and the network structure. The most analytically tractable model to incorporate a representation of the topology of the pore network is the endlessly branching network without closed loops, that is, the Bethe tree network, as shown in Figure 2.

Larson et al. (1981) used Bethe lattices to study the distribution of oil blobs in a porous medium. Other studies em-

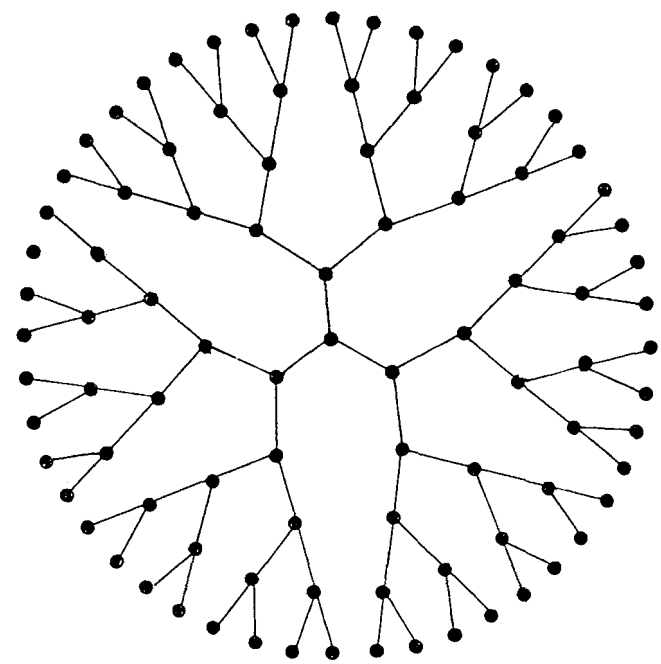

Figure 2. Bethe tree, a network model without closed loops, with connectivity $C = 3$.

ploying Bethe lattices to represent porous materials include Heiba et al. (1992) for two-phase flow, Reyes and Jensen (1985) for estimation of effective transport coefficients in modeling gas–solid reactions (Reyes and Jensen, 1986a,b; 1987), and Sahimi (1993a) in the study of nonlinear transport processes in disordered media. The behavioral study of the effective transport properties of the systems, such as permeability, conductivity, and diffusivity, shows that in all cases the concepts of percolation theory play a prominent role, even if the system is well connected and percolation may seem not to play any role (Zhang and Seaton, 1992; Sahimi, 1993a).

Models that treat the pore system in the sorbent as an interconnected network have been recently developed for adsorption–desorption equilibrium processes with hysteresis (Mason, 1988; Parlar and Yortsos, 1988, 1989; Rajniak and Yang, 1993, 1994; Sahimi, 1993b), and the Bethe tree was used as the network model in these articles. These models explain the general form of the desorption isotherm by the concept of pore blocking, where the emptying of a large pore-filled with capillary-condensed liquid is determined by the emptying of its smaller neighbors. The equilibrium behavior of capillary condensate is comparatively well understood and described, but the dynamic behavior has not been studied in these works.

One of the simplest methods for estimating the effective transport properties of disordered media is the effective-medium approximation (EMA), which is a phenomenological method by which a disordered medium is replaced with a hypothetical homogeneous one represented by unknown physical constants (Kirkpatrick, 1973; Benzoni and Chang, 1984; Burganos and Stoirchos, 1987; Burganos and Payatakes, 1992; Sahimi, 1993a,b). Thus, EMA is an ingenious way of transforming a many-body system into a one-body problem. From the solution of transport equations in the model of porous media, one obtains the desired estimates of the effective transport coefficients.

In what follows, the problem of mass transport of condensable adsorptive in the porous sorbent is studied. The primary objective of this contribution is to establish a simple theoretical framework of predicting effective diffusivity for adsorption–desorption hysteresis-dependent processes. In the next section we discuss briefly the main concepts of the equilibrium theory for the sorption systems with hysteresis (Mason, 1988; Rajniak and Yang, 1993, 1994) based on the pore-blocking theory and percolation theory in Bethe tree network. Next we develop the network model for the transport of condensable vapor in the porous sorbent based on the information from the equilibrium model. We have used the effective-medium approach to produce a method for calculating the effective diffusivity that can explain the maximum of the diffusivity or permeability in the capillary condensation region.

The second objective of this study was to provide a set of accurate experimental data for the kinetics of water vapor sorption on silica gel and to compare these data with theoretical predictions. Also some experimental data from the literature are compared with the proposed model.

Theoretical Considerations

We consider adsorption–desorption processes of condensable vapors in a porous adsorbent. During the primary adsorption the porous adsorbent initially free of adsorbate is exposed to a vapor phase at low pressure P_V. At the beginning, the vapor molecules adsorb at particular sites on the surface of the solid and eventually multilayer adsorption occurs on the pore walls, with the adsorbed layer becoming thicker. Besides gaseous diffusion and flow in pores, surface flow of physically adsorbed vapor is important. The surface diffusion can make an important contribution to the mass transfer.

To explain the surface flow, several interpretations are available. The most commonly used models are essentially divided according to the two distinct approaches: the site-hopping model (Higashi et al., 1963; Kapoor et al., 1989; Chen and Yang, 1993; Tamon et al., 1981) and the approach based on the chemical potential as the driving force (Kärger and Ruthven, 1992), which results in *approximately* (Yang, 1987) the "darken equation" as shown below. The transport equation for surface diffusion may be written in the form

$$J = -D\frac{da}{dz} \qquad D = D_0\frac{d\ln x}{d\ln a} \tag{1}$$

where J is the surface flux; D_0 is generally referred to as the "corrected diffusivity;" a is the concentration in the adsorbed phase; x is the relative pressure in the vapor phase; $x = P_0/P_{sat}$, where P_{sat} is the saturation pressure; and z is distance coordinate.

When the condensation pressure is reached in the finest pores and the multilayer becomes sufficiently thick, the pores fill with a liquidlike phase. This phase transition is known as *capillary condensation* and it commences in the finest pores at a critical pressure, P_{crit}, of the "critical" pore size (provided pores of this size are present). We will assume that the capillary condensation starts in the finest pores at point L, the lower closure point of the hysteresis loop (see Figure 1a). However, this is not necessarily so, because the closure of the hysteresis loop during the desorption process occurs when all pores containing condensate have access to the vapor phase. This may occur also above P_{crit}. In fact, condensation occurs only in pores above a critical pore size. In smaller micropores, the phase transition disappears and the micropores fill with adsorptive at a "filling pressure." This means that the position of the lower closure point L is characteristic of each adsorptive (Seaton, 1991; Burgess et al., 1989; Naono and Hakuman, 1993). As the pressure is progressively increased, wider and wider pores are filled until the saturation pressure is reached.

Mass transport in the capillary condensation regime is a complex phenomenon. The conditions under which capillary condensation occurs are also those under which significant surface diffusion is expected. The study of this phenomenon is therefore complicated by the difficulty of separating the contributions from the various transport mechanisms. Fortunately, vapor flow contribution is found to be negligible under those conditions (Haynes and Miller, 1982; Abeles et al., 1991; Tsujikawa et al., 1987). Vapor phase transport is in this case usually orders of magnitude smaller than surface flow because of the relatively small amount of molecules in the vapor phase compared to that in the adsorbed phase.

As soon as a pore is filled with condensate, the vapor flux through that pore is cut off and transport then depends on

surface diffusion together with any bulk flow induced by the capillary forces. Intuitively one might therefore expect the apparent diffusivity to be greatly reduced. However, when there is a significant distribution of pore sizes, the flux, and therefore the apparent diffusivity, may in fact be greatly enhanced. This counterintuitive result was first pointed out by Carman and Raal (1951a), and more detailed analyses have been given by Weisz (1975), Lee and Hwang (1986), Abeles et al. (1991), and Kärger and Ruthven (1992).

The capillary condensation pressure, P_v, can be estimated by the well-known Kelvin equation, which for cylindrical capillary has the form

$$\frac{P_v}{P_{\text{sat}}} = \exp\left(-\frac{2\sigma V_L \cos\theta}{rRT}\right), \tag{2}$$

where σ is the interfacial tension between liquid and gas, V_L the molar volume of the liquid adsorbate, both being functions of the absolute temperature T, P_V is the condensation pressure for the cylindrical capillary with radius r, and θ is the contact angle. A curved interface not only reduces the saturation vapor pressure but also causes a hydrostatic pressure difference across the meniscus (Carman and Raal, 1951a), via the Young–Laplace equation:

$$P_{\text{suc}} = P_L - P_v = -\frac{2\sigma\cos\theta}{r} \tag{3}$$

where the pressure in the vapor P_v exceeds that of capillary condensed (liquid) phase P_L and the difference P_{suc} is the capillary suction pressure. Combining the Young–Laplace equation (Eq. 3) with the Kelvin equation (Eq. 2), and applying for both ends of the liquid-filled part of the capillary, (Figure 3), we get the expression for the overall pressure drop in the liquid phase:

$$P_{L1} = P_{L2} = P_{v1} - P_{v2} + \frac{RT}{V_L}\ln\frac{P_{v1}}{P_{v2}}. \tag{4}$$

The driving force for the liquid flow is the sum of the vapor phase pressure drop, given by the first term on the righthand side of Eq. 4, and the capillary pressure, given by the second term. From Eq. 4 it is predicted that the actual pressure drop is much greater than the vapor phase pressure drop.

In any adjoining capillary in which condensation has not yet occurred, transport will be by surface flow only. It is clear

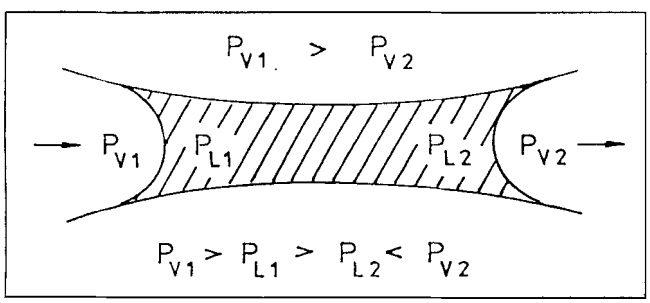

Figure 3. Pressure distribution in a single capillary partially filled with condensate (shaded area).

then that for any reasonable pressure gradient within a permeable solid, any capillary condensate volume elements will create a short-circuit effect leading to a reduction in the length of the diffusion path and a corresponding increase in the effective surface diffusivity.

Weisz (1975) proposed that if the capillary condensed volume elements represent a fraction q of the pore volume, we may expect a shortening of the diffusion path by q, the effective diffusivity will then be

$$\frac{D_{\text{eff}}}{D} \sim \frac{1}{1-q}, \tag{5}$$

where q can be estimated from the pore size distribution and from the critical Kelvin radius r given by Eq. 2.

As the relative pressure increases, the number of pores that are still not filled with condensate decreases rapidly and at the point U, the upper limiting point of the hysteresis loop, all pores are filled with capillary condensate, as seen in Figure 1a.

The position of the upper closure point U depends on the pore size distribution of the adsorbent and particularly on the size of the largest mesopores. For mesopores solids in which essentially all the pores are sufficiently small for condensation to occur at some point during the primary adsorption, there is little condensation near the saturation pressure, $x = 1$, and the point U lies below the saturation pressure (Mason, 1988; Liu et al., 1993). If point U, the upper limiting point of the hysteresis loop, lies below the saturation pressure of the adsorbate vapor, then it is presumed that the solid has no pores of radii greater than that corresponding to the closure point. Adsorption beyond this pressure will be associated with the change of curvature of menisci freely accessible to the vapor and with the compression of liquid condensate in the pores.

Transport of the liquid condensate can then occur only by hydraulic pressure, that is, capillary pressure eliminated, because the entire porous sample is filled with a bulk condensate and nowhere does a meniscus exist in the pores. The flow of the condensate obeys the Hagen–Poiseulle equation, and under usual conditions of adsorption experiments this flow is much smaller than the capillary condensate flow.

From this qualitative analysis it follows that beside surface flow of adsorbed species, other different mechanisms also influence the total mass transport rate in the capillary condensation regime. The first effect is the increase in the apparent diffusivity when some pores (or some parts of the capillary) are filled with condensate. The second effect is the decrease in the mass transport rate once all pores (or the whole capillary) are filled by condensate. With the increase of the roles of these two mechanisms, the role of surface diffusion is decreased and the dependence of the effective diffusivity on relative pressure can pass through a maximum as shown in Figure 1b. In the interconnected network of pores of various sizes all three mechanisms can be operative. For the analysis of the relative influence of each mechanism we will examine the primary desorption isotherm, Figure 1a.

The primary desorption process is the reversal of the primary adsorption, and it commences upon completion of the primary adsorption at relative pressure $x = 1$. The corre-

sponding equilibrium curve is termed primary (boundary) desorption isotherm. A characteristic feature of desorption for various sorption systems is its hysteresis loop, when the adsorbed amount between points L and U is greater at any given relative pressure x along the primary desorption curve than along the primary adsorption curve. This primary desorption loop is reproducible if the desorption process is started from any point beyond the upper limiting point U or at least from this point U, that is, for $x > x^U$.

For the present analysis the position of the closure points L and U are important. As it is already in the smallest pores above the critical pore size and at point U the capillary condensation is completed in the largest mesopores of the solid.

Following the "pore-blocking theory" of Mason (Mason, 1988; Rajniak and Yang, 1994) a porous material (adsorbent) consists of a number of pores connected together in a network. In this network we distinguish bonds (pore throats, windows) from sites (pore bodies, cavities). The individual sites are connected via bonds. Three parameters or functions characterize the pore spaces: connectivity C and site size and bond size distribution functions, $g(r)$ and $f(r)$, respectively. Connectivity is defined as the average number of bonds per pore. The characteristic dimension of the bond or of the site, r, is related to the filling pressure (capillary condensation) via the macroscopic Kelvin equation (Eq. 2) for capillary condensation. Thus, at any value of the relative pressure x ($= P_v/P_{sat}$), the process may be uniquely parameterized by a radius r, via Eq. 2. Accordingly, adsorption or desorption occurs corresponding to an increase or decrease in r, respectively.

It is worth noting that the geometric radius of a pore is the sum of the Kelvin radius plus the thickness of the adsorbed layer at the pore surface and that the generally recognized validity for the Kelvin equation is limited to the mesopore size in the range 1 nm $< r <$ 25 nm.

The distribution functions $g(r)$ and $f(r)$ are the normalized functions, such that $g(r)\,dr$ denotes the probability that a pore has a site (cavity) radius between r and $r + dr$, and similarly $f(r)\,dr$ is the probability of any bond (window) having a radius between r and $r + dr$.

The fraction of bonds for which $r < r_P$ and so represents the probability that a capillary meniscus will not pass through a window will be

$$p = \int_0^{r_P} f(r)\,dr, \tag{6}$$

and the probability that the site of the pore will be filled at the value of r_q set by P/P_{sat} will be

$$q = \int_0^{r_q} q(r)\,dr. \tag{7}$$

It should be mentioned that Mason's pore-blocking theory was developed for the hysteresis (capillary condensation) domain, and therefore describes adsorption–desorption processes only for relative pressure $x^L < x < x^U$. It follows then that $q = p = 0$ for $x \le x^U$, and $q = p = 1$ for $x \ge x^U$. The advantage of using probabilities p and q is that they make the derived functions independent of any particular pore size distribution and the analysis is thus general; the details of the size distribution and the geometry are all incorporated into the probabilities p and q.

The adsorption process in the hysteresis-dependent domain is represented by the increase of q from 0 to 1 and desorption process by the reduction of p from 1 to 0. Probabilities p and q are related through connectivity C by

$$q = p^C, \tag{8}$$

which considerably simplifies calculations (Mason, 1988; Ball and Evans, 1989; Parlar and Yortsos, 1988).

For the description of primary and secondary sorption isotherms two general variables, a and S, must be introduced. The variable a expresses the total measured amounts of adsorption or desorption (the sum of both surface adsorption and capillary condensation) in the whole range of relative pressure $0 < x < 1$, whereas the variable S represents the fraction of pores that are filled by capillary condensation. Mason assumed that there is no correlation between the cavity radius for filling and the cavity volume. This assumption enables the number fraction to become the volume fraction and it makes the analysis independent of any particular pore size distribution. More recently Mason and Mellor (1991) have shown that for a random packing of equal spheres the number fraction of pores emptied during the drainage process corresponds closely with the volume fraction of the pores. Following Parlar and Yortsos (1988) we will also expect that the capillary condensation phenomenon controls the equilibrium of the sorption processes in the range of relative pressures $x^L < x < x^U$. It has been shown by Mason (1988) and by Rajniak and Yang (1993) that the preceding assumption is fairly valid for the systems xenon on Vycor glass and water on silica gel, respectively, and the contribution from surface adsorption to the total amount is practically constant in the range $x^L < x < x^U$ and is equal to a^L. Then the fraction of pores filled, S, is related to the adsorbed amount by the following expression

$$S = \frac{a - a^L}{a^U - a^L} \quad \text{for} \quad x^L \le x \le x^U. \tag{9}$$

For the primary adsorption process (the subscript A is for primary adsorption), the fraction of pores filled by capillary condensation is

$$S_A = q \quad \text{for} \quad x^L \le x \le x^U, \tag{10}$$

where q is the probability of pore filling. It is worth noting that S_A is not dependent on the connectivity C. On adsorption, pore blocking does not play any role in adsorption equilibria. When a porous material is filled by adsorption, all of the pores are equally accessible. Even if the pore becomes isolated from the bulk vapor, it can still fill by condensing vapor from adjacent pores that can then refill from the bulk vapor. However, this process will be quicker than the filling from the vapor, as discussed earlier.

For primary desorption the hysteresis of capillary condensed vapor can be explained by pore-blocking effects, where a pore cannot empty until at least one of its neighbors has

emptied. This effect depends in principle on the interconnections and the interconnectedness of the pore network. The model frequently used for the interconnectedness is the Bethe tree (Mason, 1988; Parlar and Yortsos, 1988), the network with no closed loops (Figure 2). The advantage of using the Bethe tree is that the description of its behavior can be carried out analytically.

The sorption hysteresis is a connectivity-related phenomenon. Such phenomena are naturally described by the percolation theory (Broadbent and Hammersley, 1957; Stauffer and Aharoni, 1992; Sahimi, 1994). The analysis given here follows Mason's analysis using percolation theory with the restriction to a Bethe tree network.

During the primary desorption process whether a site remains full or empty depends upon whether one of its bonds is connected to the vapor and at the same time can also allow a capillary meniscus to pass. At some stage during primary desorption, at some value of p, the probability that a bond into a site is connected to the vapor is v. Mason (1988) derived Eqs. 11 and 12 for the fraction of the pores filled during primary desorption S (the subscript D is for primary desorption) at respective values of probabilities p and v

$$S_D = (1 - v)^{C/(C-1)} \tag{11}$$

$$p = (S_D^{1/C} - S_D^{(C-1)/C})/(1 - S_D^{(C-1)/C}). \tag{12}$$

Equations 11 and 12 predict the correct limits, $S = 1$ for $v = 0$ and $S = p = 0$ for $v = 1$. Some plots of S against p for various values of C are given in Mason's study (1988). For $C = 3$ it is easy to solve Eqs. 11 and 12 analytically.

The primary desorption equilibrium problem described previously belongs to the group of bond percolation problems, because the emptying of the pore sites (cavities) is determined by the bonds (windows) connections. Connectivity of the network plays a dominant role in the description of the process.

On the other hand, the primary adsorption process in the capillary condensation region can be treated as a classic site percolation problem. In this case pore sites (cavities) of the network are filled by capillary condensate with probability q and partially filled by surface adsorption with probability $1 - q$. As discussed earlier, whether a particular site is filled by capillary condensation or not depends only on its characteristic dimension (mean radius of curvature) r while the connectivity of the pores is irrelevant. But the physical picture is different from the point of view of kinetics of the porous adsorbent filling.

During adsorption at a partial pressure below the lower limiting point L, no pores are filled by capillary condensation. Surface diffusion controls the mass transport rate in the porous adsorbent. At relative pressures above the point L, a fraction of the pores q randomly interspersed in the sorbent are filled by capillary condensation that accelerates the total rate of mass transport (filling of the fraction $1 - q$ of the pores partially filled by surface diffusion). The rate of filling of any pore may be slower or faster, depending on the situation in the neighbors of the pore (i.e., whether these are partially filled by surface adsorption or completely filled by capillary condensation, or generally, depending on the situation in the whole network. This diffusion problem is then analogous to the conduction problem in a network of heterogeneous conductors. It has been pointed out (e.g., Sahimi et al., 1990; Stauffer and Aharony, 1992) that the exact relationship between electrical conductivity and fluid permeability of a porous medium is an unsolved problem. Similarly, the relationship between effective conductivity and effective diffusivity is not obvious. For gaseous diffusion (bulk and/or Knudsen) Burganos and Sotirchos (1987) and Burganos and Payatakes (1992) have presented a method for calculating the effective diffusivity of a porous solid based on the effective medium approximation (EMA). Liu et al. (1992) have used EMA to investigate the effect of pore geometry on the effective diffusivity. However, the effect of surface diffusion or capillary condensation was not considered in these works.

In the present contribution we propose to develop a physical model for mass transport in the porous medium in the presence of capillary condensation based on the following assumptions:

1. The pore sites (cavities) of the porous medium are filled by capillary condensation or partially filled by surface diffusion. The fraction of pores filled by capillary condensation is q and that partially filled by surface diffusion is $1 - q$.
2. We will use the symbol d_s for the diffusivity in the pore site that is partially filled by surface diffusion and symbol d_c for the "diffusivity" in the pore site that is filled by capillary condensation. Mass transport occurs in pores containing condensate by pressure-driven flow, rather than diffusion, and the use of d_c for such kind of transport is a formal simplification.
3. The bonds (pore throats, windows) between the pore sites do not contribute significantly to the total volume and the volume of capillary condensed liquid is associated only with the pore sites.

Then the problem of mass transport in the porous adsorbent with randomly distributed fractions of pores filled by capillary condensation or by surface diffusion, respectively, is similar to the problem of diffusion in bi-disperse media (Benzoni and Chang, 1984; Burganos and Sotirchos, 1987). Generally, a discrete multimodal distribution of pore diffusivities with the number density $f(d)$ of pore diffusivities has the form

$$f(d) = \sum_{i=1}^{n} f_i \delta(d - d_i), \tag{13}$$

where δ is the Delta function and d_i is the diffusivity of the pore of the ith kind (e.g., $d_i = d_s$ for the pore partially filled by surface adsorption and $d_i = d_C$ for the pore filled by capillary condensation) and n is the number of different fractions of pores. The EMA equation for the Bethe lattice with connectivity C (Stinchcombe, 1974; Heinrichs and Kumar, 1975; Sahimi, 1993a) reduces to the summation

$$\sum_{i=1}^{n} f_i \frac{d_i - d_{\mathrm{EMA}}}{d_i + (C-2)d_{\mathrm{EMA}}} = 0, \tag{14}$$

where n is the number of different fractions of pores, d_{EMA} is the effective medium diffusivity, and d_i is the diffusivity of the pore of type i. For two-dimensional or three-dimensional networks of coordination number C, an equation similar to Eq. 14 can be used (Kirkpatrick, 1973; Sahimi, 1993a) except

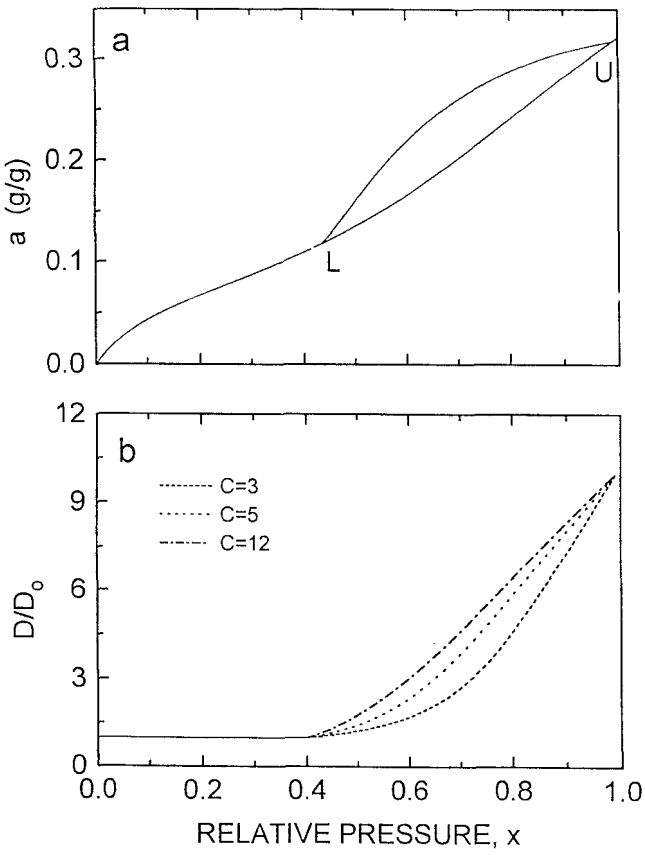

Figure 4. Theoretical predictions of diffusivity by Model 1.

(a) Adsorption–desorption equilibrium with upper closure point U close to the saturation pressure at $x = 1$. (b) Concentration dependence of diffusivity with maximum at $x = 1$ for various values of connectivity; $d_c/d_s = 10$.

that C-2 must be replaced by $(C/2-1)$. However, to maintain consistency with the network model used for evaluating connectivity from the adsorption–desorption equilibrium data (Mason, 1988; Rajniak and Yang, 1993), which is restricted to the Bethe tree network, we use the EMA given by Eq. 14.

The value of d_{EMA} computed from the effective medium equation (Eq. 14) is related to the effective diffusivity of the whole network D_{EMA} (Stinchcombe, 1974) by

$$D_{\mathrm{EMA}} = C\frac{(C-2)}{(C-1)}d_{\mathrm{EMA}}. \qquad (15)$$

The simplest model that will be discussed in the present analysis (Model 1) can be derived from Eqs. 13 and 14, and can be summarized as follows:

Model 1:

For $x \le x^L$: $f_1=1 \quad f_2=0 \quad d_{\mathrm{EMA}}=d_s$

For $x^L < x < x^U=1$: $f_1=1-q, \quad f_2=q, \quad d_1=d_s, \quad d_2=d_C$, d_{EMA} given by Eqs. A1 and A2 (Appendix).

The dependence of the effective diffusivity for Model 1 is shown in Figure 4, for various values of connectivity. In this case the upper closure point U is at relative pressure $x = 1$ and capillary condensation accelerates the mass transport rate in the whole concentration range above point L. As can be expected, the acceleration of the mass transport rate in the capillary condensation regime is more pronounced for higher values of connectivity. However, the curves for various connectivities are relatively close together, especially for C greater than 5. Such behavior is also typical for the related percolation problem of the theoretical equilibrium boundary desorption curves with various connectivities (Mason, 1988).

If the upper closure point U lies below $x = 1$, we can expect a decrease of the total mass transport rate for relative pressures $x^U < x < 1$, because in this region all pores are filled with capillary condensate and the transport is controlled by the flow of liquid condensate. For such systems a more complicated model, Model 2, is proposed:

Model 2:

For $x \le x^L$: $f_1=1 \quad f_2=0 \quad d_{\mathrm{EMA}}=d_S$

For $x^L < x < x^U$: $f_1=1-\mathrm{q} \quad f_2=q \quad d_1=d_S \quad d_2=d_C$ d_{EMA} given by Eqs. A1, A2 (Appendix)

For $x \ge x^U$: $f_1=0 \quad f_2=1 \quad d_{\mathrm{EMA}}=d_F$.

The theoretical dependence of the effective diffusivity based on Model 2 for various values of connectivities is shown in Figure 5. The upper closure point U now lies below the saturation pressure ($x^U < 1$) and the dependence of diffusivity contains a maximum at $x = x^U$. For $x > x^U$ there exists a

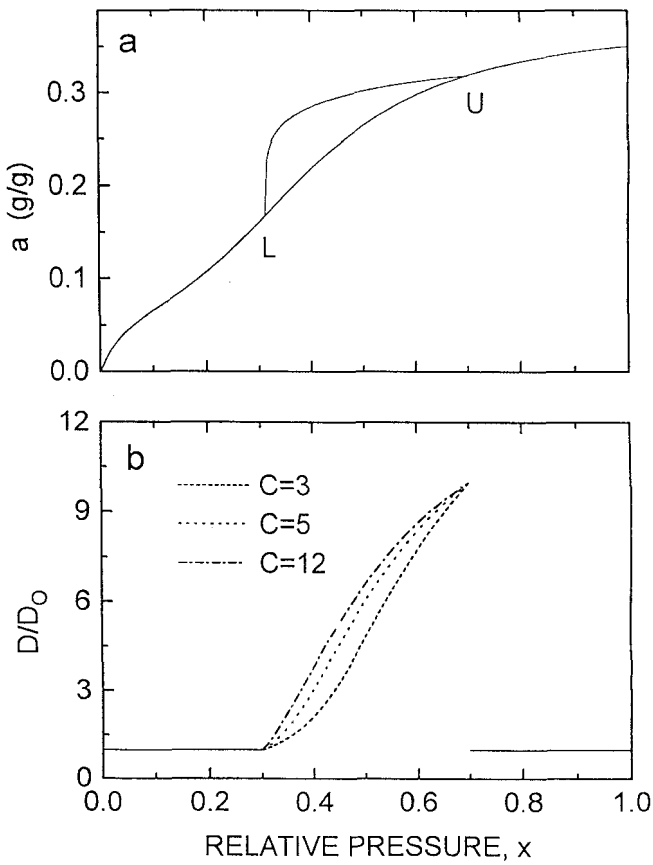

Figure 5. Theoretical predictions of diffusivity by Model 2.

(a) Adsorption–desorption equilibrium with upper closure point U at $x = 0.7$. (b) Concentration dependence of diffusivity with maximum at $x = 0.7$ for various values of connectivity; $d_S = d_F$ and $d_c/d_s = 10$.

discontinuity in the concentration dependence of diffusivity that decreases immediately to the value d_F, which is diffusivity in the pore filled by capillary condensation in the region when the whole sample is filled with condensate. In this region, the transport is controlled by the liquid flow of capillary condensate during the compression of the condensate in the sample and flattening of the menisci. Such discontinuity is an artifact of the model and needs further discussion.

The theoretical relations of Model 1 and Model 2 were developed for the idealized case of the infinite network (e.g., Bethe tree), in which there are no blind pores and the effect of decreasing the total mass transport rate by the influence of the flow of capillary condensate in pores completely filled by the condensate is important only for $x \geq x^U$. In the real porous adsorbents there definitely exist blind (dead-end) pores. These blind pores are accessible for filling by surface adsorption and capillary condensation; but after filling with capillary condensate they do not increase the total mass transport rate, but on the contrary, decrease it. It is clear that the fraction of pores that belongs to these "blind clusters" increases with increasing q, and for $q = 1$, all pores are filled with condensate and belong to blind clusters. Therefore, in real porous adsorbents with the broad pore size distribution and with presence of blind pores, all three main mechanisms (surface diffusion, capillary condensation, and liquid flow of capillary condensate) may already be functional simultaneously below the point U. In other words, the total mass transport rate (effective diffusivity) will pass a maximum at the relative pressure $x < x^U$. The position of this maximum will depend on the initial fraction of blind pores in the sample, on the connectivity as well as on the sizes of microparticles in the sorbent.

It should be noted that the fraction of blind pores in the real sorbents is different from the tag-end fraction of bonds (sites) of the theoretical (infinite) Bethe tree network that consists of a fraction q of conducting bonds (sites) and a fraction $1 - q$ of nonconducting bonds (sites) (Larson and Davis, 1982). The relations of Larson and Davis for the tag-end fractions (backbone fractions) of bonds (similarly for sites) were developed to study a conduction problem for systems in which there were two types of sites—conducting (occupied) and nonconducting (unoccupied). They represent the fraction of the occupied sites that belong to an infinite cluster of occupied sites but do not carry current (flow), they are dead-end, that is, connected with one (and only one) of the bonds to the infinite cluster. The tag-end fraction defined in such a way decreases with increasing q. Our problem is different, however, because we expect that all pores are conducting. But the occupied sites (sites filled with capillary condensation) with connections to unoccupied sites are conducting differently from both the unoccupied sites (i.e., partially filled with surface adsorption) and the occupied sites that have no connections to the unoccupied sites. The fraction of blind pores filled with capillary condensate will in our case increase with increasing q.

The relative pressure x^* (or the corresponding fraction of pores filled, q^*) at which the blind pores become filled with capillary condensate can be considered important only empirically on the basis of the experimental position of the maximum diffusivity. Following the ideas presented earlier we have Model 3 incorporating the influences of all three main mechanisms that determine the total mass transport rate in the porous structure:

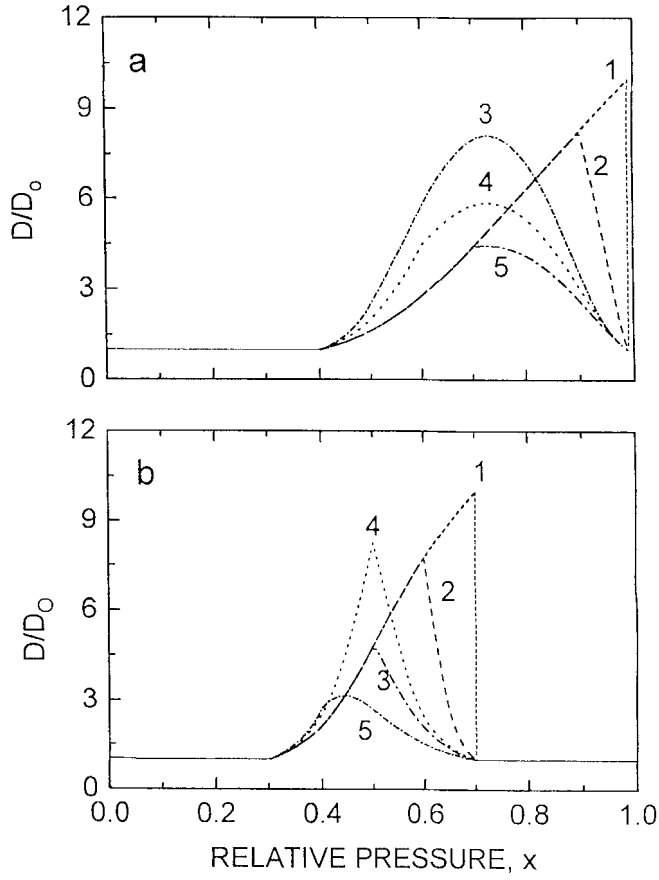

Figure 6. Theoretical predictions of diffusivity by Model 3 for various values of the ratio d_C/d_S and various values of the empirical relative pressure x^* (defined in the text).

(a) Concentration dependence of diffusivity for equilibrium shown in Figure 4a for $c = 8$ and $d_S = d_F$. 1: $d_C/d_S = 10$, $x^* = 0.99$; 2: $d_C/d_S = 10$, $x^* = 0.9$; 3: $d_C/d_S = 40$, $x^* = 0.5$; 4: $d_C/d_S = 20$, $x^* = 0.6$; 5: $d_C/d_S = 10$, $x^* = 0.7$. (b) Concentration dependence of diffusivity for equilibrium shown in Figure 5a for $C = 3$ and $d_S = d_F$. 1: $d_C/d_S = 10$, $x^* = 0.7$; 2: $d_C/d_S = 10$, $x^* = 0.6$; 3: $d_C/d_S = 10$, $x^* = 0.5$; 4: $d_C/d_S = 20$, $x^* = 0.5$; 5: $d_C/d_S = 30$, $x^* = 0.4$.

Model 3:

For $x \leq x^L$: $f_1 = 1 \quad f_2 = f_3 = 0 \quad d_{EMA} = d_S$

For $x^L < x^* < x^U$: $f_1 = 1 - q \quad f_2 = q(1 - s) \quad f_3 = q_S$
$d_1 = d_S \quad d_2 = d_C \quad d_3 = d_F$
d_{EMA} given by Eqs. A4 and A5 (Appendix)

For $x \geq x^U$: $f_1 = f_2 = 0 \quad f_3 = 1 \quad d_{EMA} = d_F$.

The fraction of blind pores filled with capillary condensate, s, is defined by:

$$s = \frac{a - a^*}{a^U - a^*} \tag{17}$$

and the solution of Eq. 14 for Model 3 is given in the Appendix.

In Figure 6 the theoretical dependences of diffusivity computed via Model 3 are shown for various values of x^* and

various values of the ratio d_C/d_S. For simplicity, we expected $d_S = d_F$ in all cases. In Figure 6a, the theoretical curves are presented for the system with equilibrium shown in Figure 4a (water vapor in alumina, $C = 8$). Curve 1 represents the limiting case of Model 1 for $x^* = x^U$, that is, $q^* = 1$. Curves 2 and 5 show the effect of the decreasing value of x^* on the position and the height of the maximum for the same value of the ratio d_C/d_S. Curves 3 and 4 demonstrate the influence of the simultaneously increasing value of the ratio d_C/d_S and decreasing value of x^*. One interesting feature of the model is the constant position of the rounded maximum for Curves 3, 4, and 5. For these cases $q^* < 1/2$ and the maximum is at x corresponding to $q = 1/2$. For the cases with $q^* > 1/2$ the corresponding position of the sharp maximum is always at q^*. Similar conclusions are valid for the system shown in Figure 6b, where the theoretical curves for the system with equilibrium shown in Figure 5a (water vapor in silica gel, $C = 3$) are presented.

Experimental

Two standard commercial dessicants, silica gel Davison Grade H and activated alumina Alcoa PSD-350, were used in experiments. Adsorption data for nitrogen at the liquid nitrogen temperature, 77 K, were obtained using a Carlo Erba Sorptomatic 1900 apparatus and have shown complete reversibility through the entire pressure range. The specific BET surface area and pore volume for Grade 12 silica gel were determined to be 767 m^2/g and 0.398 cm^3/g, respectively. This silica gel was microporous with a mean pore width of 0.9 nm and the largest pores of about 1.6 nm (Rajniak and Yang, 1993). Results for activated alumina have shown a significant hysteresis loop in the N_2 relative pressure range of 0.42–0.99. The BET surface area and pore volume were 350 m^2/g and 0.59 cm^3/g, respectively.

Equilibrium and kinetic data were measured using a Mettler TA2000C Thermoanalyzer (TGA). High-purity helium was used as the inert carrier gas and the gas for regeneration. The generation of water vapor at the desired partial pressure was accomplished with the aid of a gas washbottle containing distilled water, two cylinders of helium gases, flowmeters, and a gas blending system (Yang and Baksh, 1991). By controlling both the flow rate of helium through the washbottle and the flow rate of the diluting helium, the concentration was varied to obtain the entire adsorption isotherm.

For the kinetic data measurement the flow system was slightly modified to avoid the influence of the external diffusion during uptake experiments. The total flow rate of the mixture flowing to the TGA was increased by using two additional gas washbottles. The experimental conditions were adjusted to ensure that the external diffusion resistance was absent (or minimized to a negligible level) and that the wet helium stream was indeed saturated. The partial pressure of water in helium gas flowing to the TGA was changed by varying the ratio of the flow rate of pure helium to the helium saturated with water, keeping the total flow rate constant. Equilibrium data obtained using the extended flow system are in good agreement with the data reported in our previous works (Rajniak and Yang, 1993, 1994).

The TGA microbalance measured weight changes of the adsorbent accurately up to 10 μg. The adsorptive entered through the TGA inlet, and flowed over the adsorbent and the sample pan before exiting.

The silica gel sample was activated by passing high-purity helium through it for 2 hours at 200°C. The first adsorption isotherm was measured at 25°C up to the saturation relative pressure. After the adsorbent was exposed to water vapor at the saturation pressure for 6 hours, the first desorption was carried out by passing pure helium through the sample. The weight of the rehydroxylated sample was taken as the basis for sorption data evaluation.

In the diffusivity measurement, the sample initially at equilibrium was subjected to a sudden small change in partial pressure and the weight changes during adsorption or desorption were continually recorded. The influence of the external diffusion was minimized by using a high total flowrate of the mixture flowing to the TGA as discussed. The heat effects during the sorption measurements were minimized by allowing only small step changes in relative pressure during each measurement. Because the sorption rates were independent of the pellet size, we can assume that the total sorption rate for water in silica gel was controlled by the mass transport processes within the microparticles. Successive adsorptions and desorptions were conducted at 25°C by changing the composition of the adsorptive and allowing time to establish equilibrium.

Results and Discussion

Both kinetic and equilibrium data were obtained using the experimental procedure described earlier for two silica gels. However, the kinetic and equilibrium data for the two gels are identical within the range of expected experimental error. Therefore only the results for Grade 12, which was also used in our previous works (Rajniak and Yang, 1993, 1994), will be discussed here. The equilibrium experimental data exhibited a well-behaved and reproducible hysteresis loop in the range of relative pressures 0.3–0.7, with the primary adsorption isotherm of type IV and primary desorption hysteresis loop of type H2 (IUPAC classification), shown in Figure 6. These data are in good agreement with the equilibrium data reported in our previous works (Rajniak and Yang, 1993, 1994). The primary adsorption equilibrium data were fitted by using the BDDT equation (Brunauer et al., 1940):

$$\frac{a}{a_m} = \frac{cx[1+N(G-1)x^{N-1}+(N-1-2NG)x^N+NGx^{N+1}]}{(1-x)[1-x+cx-c(1-G)x^N-cGx^{N+1}]} \tag{18}$$

A further improvement of the data fit by using the BDDT isotherm was achieved as compared to the fit by a two-site Dubinin–Radushkevich equation that was used earlier (Rajniak and Yang, 1994). The same evaluation procedure was used for the equilibrium data of water vapor on activated alumina that exhibited a significant hysteresis loop in the range of relative pressures 0.4–0.99, similar in both shape and position with the hysteresis loop for nitrogen. On the other hand, as was mentioned earlier, the adsorption–desorption equilibria on silica gel did not show any hysteresis for nitrogen but did for water. Such an interesting behavior has been explained by Naono and Hakuman (1993). For the

Table 1. Equilibrium Parameters for Sorption Systems

Sorption System	a_m	c	N	G	x^L	x^U	C
H_2O/silica gel	0.0876	17.24	4.30	21.92	0.304	0.696	3
H_2O/alumina	0.0767	9.46	8.01	0.478	0.435	0.990	8
CF_2Cl_2/Linde silica	0.1227	25.48	12.50	0.509	0.525	0.951	8

smaller molecules of water vapor (size 0.23 nm), the capillary condensation began from the pore radius of 0.9–1.1 nm, but for the larger molecules of nitrogen (size 0.36 nm) the same phenomenon started from the pore radius 1.7 nm. Because the silica gel used in our experiments was a microporous one with a mean pore width of approximately 0.9 nm and the largest pores to have a width of approximately 1.6 nm (Rajniak and Yang, 1993), capillary condensation could not occur. On the other hand, in the mesoporous alumina with a mean pore size of 3.3 nm, there was enough space for the larger molecules of nitrogen to condense.

For the purpose of quantitative evaluation of the primary adsorption kinetic data presented in this study, the positions of the limiting points of the main hysteresis loop and the value of connectivity are needed and are presented in Table 1. Connectivity C was evaluated following Mason's method (Mason, 1988; Rajniak and Yang, 1993) from the boundary desorption isotherm. The parameters of the BDDT equation are also given in Table 1.

If the uptake occurs over a small step change in the adsorbed phase concentration and with sufficiently high total flow rate, we may assume the absence of external heat and mass-transfer resistances as well as isothermal behavior during the sorption. Then the mass transport of condensable water in a spherical microparticle (radius R_p) can be represented by the following transient diffusion equation (Fick's second law) with a constant diffusivity (Kärger and Ruthven, 1992):

$$\frac{\partial a}{\partial t} = D\left(\frac{\partial^2 a}{\partial^2 r_p} + \frac{2}{r_p}\frac{\partial a}{\partial r_p}\right). \tag{19}$$

For a step change in concentration at time zero, the initial and boundary conditions are

$$t < 0, \quad a = a_0 \quad \text{(independent of } r_p \text{ and } t) \tag{20}$$

$$t \geq 0, \quad a(R_p, t) = a_\infty \tag{21}$$

$$\text{for all } t \text{ and } r_p = 0, \quad \frac{\partial a}{\partial t} = 0. \tag{22}$$

The analytical solution for Eqs. 19–21 is well known, and the Fickian diffusivity D may be determined by matching the experimental uptake curve to the solution of the diffusion equation for both adsorption and desorption experiments. A standard regression procedure was used for this purpose, using 20 experimental points for fitting the theoretical curve to each experimental transient.

The experimental results for the silica gel–water vapor system at 298 K are compared in Figure 7 with the predictions from Model 3. The equilibrium data (Rajniak and Yang, 1993), Figure 7a, exhibited a type IV isotherm for the primary adsorption isotherm and type H2 for the primary desorption hysteresis loop, with the position of the upper closure point U below the saturation pressure, that is, at $xU = 0.7$. The resulting parameters for the primary adsorption–desorption data (Rajniak and Yang, 1993) are summarized in Table 1. The value of connectivity, $C = 3$, was used to compare the theoretical concentration dependence with the experimental values. The experimental concentration dependence of the effective diffusivity shows a maximum close to the upper closure point U. From theoretical analysis, is becomes clear that for a system with such a small value of connectivity, both Model 2 and Model 3 are suitable. The effect of the finite size of the network, as well as the concentration dependence of the diffusivities (e.g., via Eq. 1 for surface diffusivity) should cause the predicted maximum to be rounded and hence improve the agreement between theory and experiment.

In Figure 8 the experimental data for the system water vapor in activated alumina are compared with the predictions

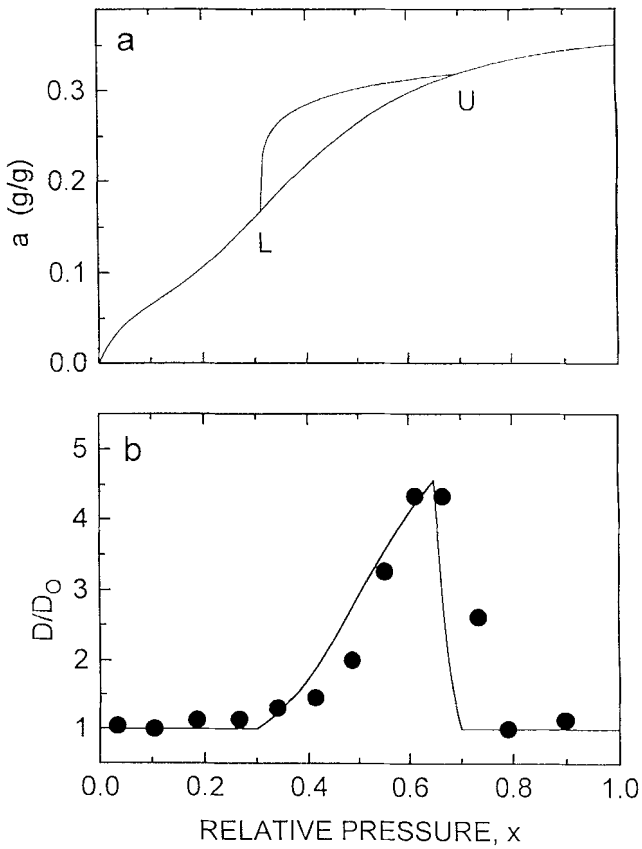

Figure 7. Experimental diffusivity data vs. theoretical predictions for the system water vapor-silica gel at 298 K.

(a) Adsorption–desorption equilibrium. (b) Concentration dependence of diffusivity, Model 3 with $C = 3$, $d_S = d_F$, $d_C/d_S = 5$, and $x^* = 0.65$.

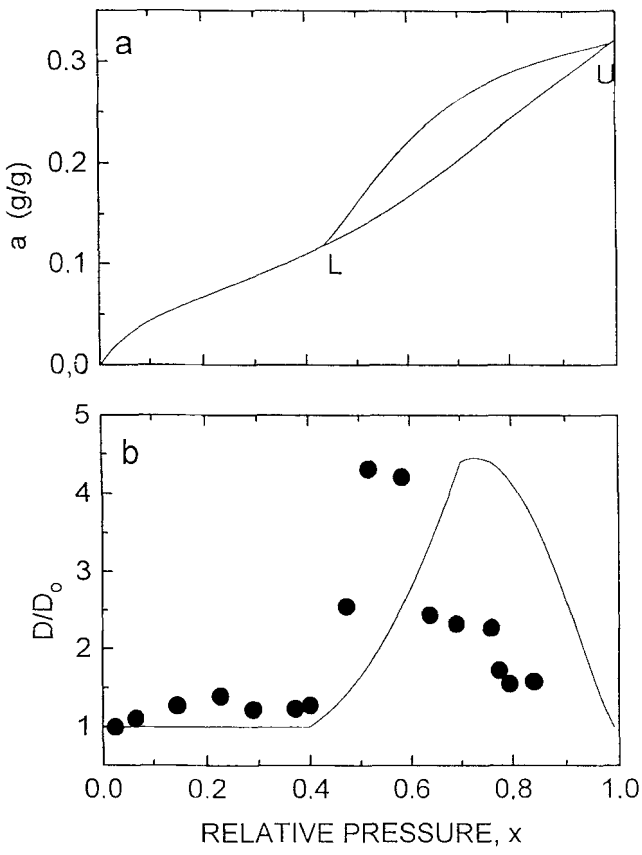

Figure 8. Experimental diffusivity data vs. theoretical predictions for the system water vapor-activated alumina at 298 K.

(a) Adsorption–desorption equilibrium. (b) Concentration dependence of diffusivity, Model 3 with $C = 8$, $d_S = d_F$, $d_C/d_S = 10$, and $x^* = 0.7$.

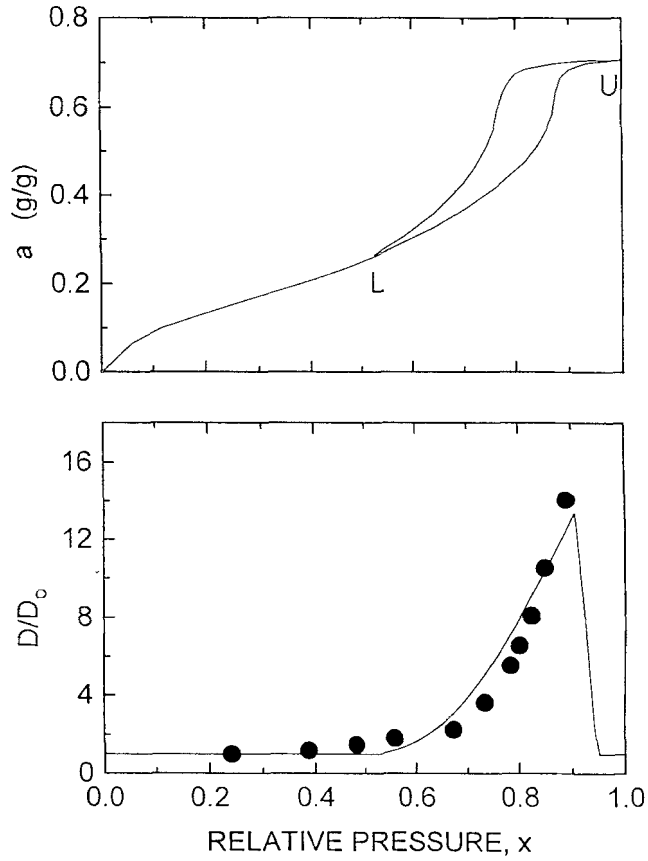

Figure 9. Experimental diffusivity data vs. theoretical predictions for the system CF_2Cl_2–Linde silica at 240 K.

From Carman (1952), Carman and Raal (1951a,b), Carman and Malherbe (1950).
(a) Adsorption–desorption equilibrium. (b) Concentration dependence of diffusivity, Model 3 with $C = 8$, $d_S = d_F$, $d_C/d_S = 20$, and $x^* = 0.88$.

by Model 3. The alumina has a well-connected structure, with $C = 8$, and exhibits a wide and smooth hysteresis loop (Figure 8a). Consequently, the model predicts a diffusivity maximum at a relative pressure substantially below the upper closure point. The experimental diffusivity maximum occurs at a relative pressure that falls further below the theoretical prediction. The agreement is, however, satisfactory judging from the simplicity of the theory.

In Figure 9 the classic experimental data of Carman and coworkers (Carman, 1952; Carman and Raal, 1951a,b; Carman and Malherbe, 1950) for system CF_2Cl_2 in a Linde silica gel at 240 K are compared with the prediction of Model 3. The equilibrium experimental data are again of type IV for the primary adsorption isotherm and type H2 for the primary desorption loop, but with the upper closure point U close to the saturation pressure $x = 1$. The parameters of the primary equilibrium data based on our evaluation are given in Table 1. The concentration dependence of the effective diffusivity is monotonically increasing in the whole reported concentration rate. Unfortunately, their last experimental diffusivity data point stops at relative pressure 0.8. However, even the simplest Model 1 can predict successfully the experimental results, as seen in Figure 9b. Moreover, it is predicted that the diffusivity will decrease at relative pressures higher than 0.88.

Experimental data for diffusivities on other vapor-porous solid systems in the capillary condensation regime are also available (Eberly and Vosberg, 1965; Rhim and Hwang, 1975; Lee and Hwang, 1985; Uhlhorn et al., 1992). These data also exhibit diffusivity maxima. However, they cannot be compared with predictions from our models because either equilibrium isotherm data are missing or only primary adsorption isotherms are available. For theoretical predictions, the primary desorption isotherm and the closure points of the main hysteresis loop are needed.

It is worth noting that Models 1–3 predict the diffusivity maximum for systems with capillary condensation in the range of relative pressures corresponding to fractional surface coverages $\theta \gg 1$. For the experimental data presented here, the values of θ at the maximum diffusivity are $\theta = 3.42$ for the water–silica gel system, $\theta = 2.35$ for the water–activated alumina system, and $\theta = 5.30$ for the CF_2Cl_2–Linde silica system. Such positions of the maxima are different from the well-known maxima for pure surface diffusion that exist at surface coverages close to 1 and that can be successfully predicted by the hopping model based on the kinetic theory (Higashi et al., 1963; Chen and Yang, 1993). For our experimental data, the maximum at θ close to 1 exists for the water-activated alumina, as shown in Figure 8. However, using the corrected diffusivity defined by Eq. 1, this maximum can

be significantly suppressed. For the water–silica gel system, no maximum is found at θ close to 1. For this system with nearly linear isotherm at low relative pressures, the Fickian surface diffusivity is practically identical to the corrected diffusivity. For the CF_2Cl_2–Linde silica system, diffusivity data are not available for low relative pressures.

Conclusion

A simple network theory is formulated for the prediction of the concentration dependence of the Fickian diffusivity for systems with capillary condensation, that is, for systems with hysteresis-dependent adsorption-desorption equilibria. The resulting models unify the equilibrium theory based on the pore-blocking interpretation of hysteresis (Mason, 1988; Rajniak and Yang, 1993, 1994) and the percolation model of mass transport in the network of pores randomly filled by capillary condensate or surface adsorption. The Bethe tree network is used to represent the topology of the network, and the effective medium approximation is employed to express the effective Fickian diffusivity during adsorption. The main advantages of the proposed models can be summarized as follows:

1. The connectivity of the porous media evaluated from the equilibrium data is taken into account.

2. The models are general for any pore geometry, and no pore size distribution data are necessary, because all relevant information is obtained from the q function, which is in fact the integral of the pore size distribution function.

3. The theory is simple to use, because of the simplicity of EMA, and the theory can be readily extended to include more transport models (Lee and Hwang, 1986).

4. The models can be further improved by allowing the diffusivities to be dependent on concentration (for example, for surface diffusivity using chemical potential as the driving force) and on pore size (for capillary condensation and flow of capillary condensate).

Acknowledgment

This work was supported by National Science Foundation grant CTS 9212279 and a grant from the National Research Council COBASE Program.

Notation

a = amount adsorbed (g/g)
a_m = parameter of BDDT equation, Eq. 18 (monolayer capacity)
c = parameter of BDDT equation, Eq. 18 (Henry's coefficient)
C = connectivity
d = diffusivity in the pore
D = diffusivity in the network (sample)
D_0 = corrected diffusivity, Eq. 1
$f(r)$ = bond radius distribution function
$g(r)$ = site radius distribution function
G = parameter of BDDT equation, Eq. 18 (energy of adsorption term)
n = number of pore fractions
N = parameter of BDDT equation, Eq. 18 (number of monolayers at saturation)
p = probability, Eq. 6
P = absolute pressure in the vapor phase
P_{sat} = saturation pressure
P_{suc} = suction pressure
q = probability, Eq. 7
r = bond or site radius of curvature
r_p = radial coordinate in the spherical microparticle
s = fraction of blind pores defined by Eq. 17
S = fraction of pores filled
v = probability that a bond is connected to the vapor during primary desorption

Subscripts

A = primary adsorption
C = capillary condensation
D = primary desorption
F = flow of capillary condensate
L = liquid
S = surface diffusion
V = vapor
EMA = effective medium approximation

Superscripts

L = lower limiting (closure) point of hysteresis loop
U = upper limiting (closure) point of hysteresis loop

Literature Cited

Abeles, B., L. F. Chen, J. W. Johnson and J. M. Drake, "Capillary Condensation and Surface Flow in Microporous Vycor Glass," *Israel J. Chem.*, **31**, 99 (1991).

Ball, P. C., and R. Evans, "Temperature Dependence of Gas Adsorption on a Mesoporous Solid: Capillary Criticality and Hysteresis," *Langmuir*, **5**, 714 (1989).

Benzoni, J., and H. C. Chang, "Effective Diffusion in Bi-disperse Media—An Effective Medium Approach," *Chem. Eng. Sci.*, **39**, 161 (1984).

Broadbent, S. R., and J. M. Hammersley, "Percolation Processes: I. Crystals and Mazes," *Proc. Camb. Philos. Soc.*, **53**, 629 (1957).

Brunnauer, S., L. S. Deming, W. E. Deming, and E. Teller, "On a Theory of the van der Waals Adsorption of Gases," *J. Amer. Chem. Soc.*, **62**, 1723 (1940).

Burganos, V. N., and S. V. Sotirchos, "Diffusion in Pore Networks: Effective Medium Theory and Smooth Field Approximation," *AIChE J.*, **33**, 1678 (1987).

Burganos, V. N., and A. C. Payatakes, "Kundsen Diffusion in Random and Correlated Networks of Constricted Pores," *Chem. Eng. Sci.*, **47**, 1383 (1992).

Burgess, C. G. V., D. H. Everett, and S. Nuttall, "Adsorption Hysteresis in Porous Materials," *Pure Appl. Chem.*, **61**, 1845 (1989).

Carman, P. C., "Diffusion and Flow of Gases and Vapours Through Micropores: IV. Flow of Capillary Condensate," *Proc. R. Soc. London*, **A211**, 526 (1952).

Carman, P. C., and P. le R. Malherbe, "Diffusion and Flow of Gases and Vapours Through Micropores II. Surface Flow," *Proc. R. Soc. London*, **A203**, 165 (1950).

Carman, P. C., and F. A. Raal, "Diffusion and Flow of Gases and Vapours through Micropores: III. Surface Diffusion Coefficients and Activation Energies," *Proc. R. Soc. London*, **A209**, 38 (1951a).

Carman, P. C., and F. A. Raal, "Physical Adsorption of Gases on Porous Solids: I. Comparison of Loose Powder and Porous Plugs," *Proc. R. Soc. London*, **A209**, 59 (1951b).

Chen, Y. D., and R. T. Yang, "Surface Diffusion of Multilayer Adsorbed Species," *AIChE J.*, **39**, 599 (1993).

Eberly, P. E., and D. B. Vosberg, "Diffusion of Benzene and Inert Gases Through Porous Media at Elevated Temperatures and Pressures," *Trans. Faraday Soc.*, **61**, 2724 (1965).

Feng, S., B. I. Halperin, and P. N. Sen, "Transport Properties of Continuum Systems Near the Percolation Threshold," *Phys. Rev. B.*, **35**, 197 (1987).

Flood, E. A., R. H. Tomlinson, and A. E. Leger, "The Flow of Fluids Through Activated Carbon Rods III. The Flow of Adsorbed Fluids," *Can. J. Chem.*, **30**, 389 (1952).

Gilliland, E. R., R. F. Baddour, and J. L. Russell, "Rates of Flow Through Microporous Solids," *AIChE J.*, **4**, 90–96 (1958).

Gregg, S. J., and K. S. Sing, *Adsorption Surface Area and Porosity*, 2nd ed., Academic Press, London (1982).

Haynes, J. M., and R. J. Miller, "Surface Diffusion and Viscous Flow During Capillary Condensation," *Adsorption at the Gas-Solid and Liquid-Solid Interface*, J. Rouquerol and K. S. W. Sing, eds., Elsevier, Amsterdam, p. 439 (1982).

Heiba, A. A., M. Sahimi, L. E. Scriven, and H. T. Davis, "Percolation Theory of Two-Phase Relative Permeabilities," SPE Meeting Paper No. 11015, New Orleans (1982).
Heinrichs, J., and N. Kumar, "Simple Exact Treatment of Conductance in a Random Bethe Lattice," *J. Phys. C.: Solid State Phys.*, **8**, L510 (1975).
Higashi, K., H. Ito, and J. Oishi, "Surface Diffusion Phenomena in Gaseous Diffusion, I. Surface Diffusion of Pure Gas," *J. Atom. Energy Soc. Japan*, **5**, 846 (1963).
Kapoor, A., R. T. Yang, and C. Wong, "Surface Diffusion," *Catal. Rev. Sci. Eng.*, **31**, 129 (1989).
Kärger, J., and D. M. Ruthven, *Diffusion in Zeolites and Other Microporous Solids*, Wiley, New York (1992).
Kirkpatrick, S., "Classical Transport in Disordered Media: Scaling and Effective-Medium Theories," *Phys. Rev. Lett.*, **27**, 1722 (1971).
Kirkpatrick, S., "Percolation and Conduction," *Rev. Mod. Phys.*, **45**, 574 (1973).
Larson, R. G., and H. T. Davis, "Conducting Backbone in Percolating Bethe Lattices," *J. Phys. C.: Solid State Phys.*, **15**, 2327 (1982).
Larson, R. G., L. E. Scriven, and H. T. Davis, "Percolation Theory of Two Phase Flow in Porous Media," *Chem. Eng. Sci.*, **36**, 57 (1981).
Lee, K. H., and S. T. Hwang, "The Transport on Condensable Vapors Through a Microporous Vycor Glass Membrane," *J. Colloid Interf. Sci.*, **110**, 544 (1986).
Liu, H., L. Zhang, and N. A. Seaton, "Determination of the Connectivity of Porous Solids from Nitrogen Sorption Measurements: II. Generalization," *Chem. Eng. Sci.*, **47**, 4393 (1992).
Liu, H., L. Zhang, and N. A. Seaton, "Analysis of Sorption Hysteresis in Microporous Solids Using a Pore Network Model," *J. Colloid Interf. Sci.*, **156**, 285 (1993).
Mason, G., "Determination of the Pore-Size Distribution and Pore-Space Interconnectivity of Vycor Porous Glass from Adsorption-Desorption Hysteresis Capillary Condensation Isotherms," *Proc. R. Soc. London*, **A415**, 453 (1988).
Mason, G., and D. V. Mellor, "Analysis of the Percolation Properties of a Real Porous Material," in *Characterization of Porous Solids II*, F. Rodriguez-Reinoso, J. Rouquerol, and K. S. W. Sing, eds., Elsevier, Amsterdam, p. 41 (1991).
Naono, H., and M. Hakuman, "Analysis of Porous Texture by Means of Water Vapor Adsorption Isotherm with Particular Attention to Lower Limit of Hysteresis Loop," *J. Colloid Interf. Sci.*, **158**, 19 (1993).
Parlar, M., and Y. C. Yortsos, "Percolation Theory of Vapor Adsorption-Desorption Processes in Porous Materials," *J. Colloid Interf. Sci.*, **124**, 162 (1988).
Parlar, M., and Y. C. Yortsos, "Nucleation and Pore Geometry Effects in Capillary Desorption Processes in Porous Media," *J. Colloid Interf. Sci.*, **132**, 425 (1989).
Rajniak, P., and R. T. Yang, "A Simple Model and Experiments for Adsorption-Desorption Hysteresis: Water Vapor on Silica Gel," *AIChE J.*, **39**, 774 (1993).
Rajniak, P., and R. T. Yang, "Hysteresis-Dependent Adsorption-Desorption Cycles: Generalization for Isothermal Conditions," *AIChE J.*, **40**, 913 (1994).
Reyes, S., and K. F. Jensen, "Estimation of Effective Transport Coefficients in Porous Solids Based on Percolation Concepts," *Chem. Eng. Sci.*, **40**, 1723 (1985).
Reyes, S., and K. F. Jensen, "Percolation Concepts in Modelling of Gas-Solid Reactions: I. Application to Char Gasification in the Kinetic Regime," *Chem. Eng. Sci.*, **41**, 333 (1986a).
Reyes, S., and K. F. Jensen, "Percolation Concepts in Modelling of Gas-Solid Reactions: II. Application to Char Gasification in the Diffusion Regime," *Chem. Eng. Sci.*, **41**, 345 (1986b).
Reyes, S., and K. F. Jensen, "Percolation Concepts in Modelling of Gas-Solid Reactions: III. Application to Sulfation of Calcined Limestone," *Chem. Eng. Sci.*, **42**, 565 (1987).
Rhim, H., and S. T. Hwang, "Transport of Capillary Condensate," *J. Colloid Interface Sci.*, **52**, 174 (1975).
Sahimi, M., "Diffusion-Controlled Reactions in Disordered Porous Media: I. Uniform Distribution of Reactants," *Chem. Eng. Sci.*, **43**, 2981 (1988).
Sahimi, M., "Nonlinear Transport Processes in Disordered Media," *AIChE J.*, **39**, 369 (1993a).
Sahimi, M., "Flow Phenomena in Rocks: From Continuum Models, to Fractals, Percolation, Cellular Automata and Simulated Annealing," *Rev. Mod. Phys.*, **65**, 1393 (1993b).
Sahimi, M., *Applications of Percolation Theory*, Taylor & Francis, London (1994).
Sahimi, M., G. R. Gavalas, and T. T. Tsotsis, "Statistical and Continuum Models of Fluid-Solid Reactions in Porous Media," *Chem. Eng. Sci.*, **45**, 1443 (1990).
Seaton, N. A., "Determination of the Connectivity of Porous Solids from Nitrogen Sorption Measurements," *Chem. Eng. Sci.*, **46**, 1895 (1991).
Stauffer, D., and A. Aharony, *Introduction to Percolation Theory*, 2nd ed., Taylor & Francis, London (1992).
Stinchcombe, R. B., "Conductivity and Spin-Wave Stiffness in Disordered Systems—An Exactly Soluble Model," *J. Phys. C.: Solid State Phys.*, **7**, 179 (1974).
Tamon, H., M. Okazaki, and R. Toei, "Flow Mechanism of Adsorbate Through Porous Media in Presence of Capillary Condensation," *AIChE J.*, **27**, 271 (1981).
Toei, R., H. Imakoma, H. Tamon, and M. Okazaki, "Water Transfer Coefficient in Adsorptive Porous Body," *J. Chem. Eng. Japan*, **16**, 364 (1983).
Tsujikawa, H., T. Osawa, and H. Inoue, "Separation of Benzene and Nitrogen by Permeation Through Porous Vycor Glass," *Int. Chem. Eng.*, **27**, 479 (1987).
Uhlhorn, R. J. R., K. Keizer, and A. J. Burgraaf, "Gas Transport and Separation with Ceramic Membranes I. Multilayer Diffusion and Capillary Condensation," *J. Memb. Sci.*, **66**, 259 (1992).
Weisz, P. B., "Diffusion Transport in Chemical Systems—Key Phenomena and Criteria, Berichte der Bunsen-Gesselschaft," *Phys. Chem.*, **79**, 798 (1975).
Yang, R. T., *Gas Separation by Adsorption Processes*, Butterworth, Boston (1987).
Yang, R. T., J. B. Fenn, and G. L. Haller, "Modification of the Higashi Model for Surface Diffusion," *AIChE J.*, **19**, 1052 (1973).
Yang, R. T., and M. S. A. Baksh, "Pillared Clays as a New Class of Sorbents for Gas Separation," *AIChE J.*, **37**, 679 (1991).
Zhang, L., and N. A. Seaton, "Prediction of the Effective Diffusivity in Pore Networks Close to a Percolation Threshold," *AIChE J.*, **38**, 1816 (1992).

Appendix

For Model 2 we need the solution of Eq. 14 for $n = 2$. The solution of the quadratic equation is

$$d_{\mathrm{EMA}} = \frac{-b + \sqrt{b^2 + 4(C-2)d_S d_C}}{2(C-2)}, \tag{A1}$$

where

$$b = d_C(1 + q - qC) + d_S(2 - q - C + qC). \tag{A2}$$

For Model 3 the solution of Eq. 14 for $n = 3$ leads to the following cubic equation

$$d_{\mathrm{EMA}}^3 + a_1 d_{\mathrm{EMA}}^2 + a_2 d_{\mathrm{EMA}} + a_3 = 0, \tag{A3}$$

which has the following solution

$$d_{\mathrm{EMA}} = 2\sqrt{-Q}\cos(\beta/3) - a_1/3, \tag{A4}$$

where

$$\cos\beta = R/\sqrt{-Q^3}; \quad Q = \frac{3a_2 - a_1^2}{9}; \quad R = \frac{9a_1a_2 - 27a_3 - 2a_1^3}{54}. \tag{A5}$$

Manuscript received Nov. 14, 1994, and revision received Apr. 24, 1995.